Engineering Structures 219 (2020) 110756

Contents lists available at ScienceDirect

Engineering Structures

journal homepage: www.elsevier.com/locate/engstruct

Vibration serviceability of a GFRP railway crossing due to pedestrians and train excitation

J.M. Russell[a,*], X. Wei[b], S. Živanović[c], C. Kruger[d]

[a] School of Engineering, University of Warwick, Coventry CV4 7AL, UK
[b] School of Civil Engineering, Central South University, Changsha 410075, China
[c] College of Engineering, Mathematics and Physical Sciences, University of Exeter, Exeter EX4 4QF, UK
[d] NOV Fiber Glass Systems, Pipex Ltd, Devon Enterprise Facility, 1 Belliver Way, Roborough, Plymouth PL6 7BP, UK

ARTICLE INFO

Keywords:
Human-induced vibration
Train buffeting
Bridge dynamics
Glass fibre-reinforced polymer

ABSTRACT

Glass Fibre-Reinforced Polymers (GFRPs) are a popular option for pedestrian bridges over railway lines as they cause little disruption for installation or maintenance. However, as they are typically lighter and less stiff than traditional materials there is concern about their dynamic response due to human induced actions and train buffeting. Due to a lack of experimental information, further data is needed if such bridges are to be used on future lines, especially with higher speed limits. This paper presents an experimental investigation of the response of a 14.5 m GFRP truss bridge due to pedestrian loading and train induced vibrations. Vibration modes of interest were identified from impact hammer tests. The vibration responses to a range of human loading scenarios, as well as multiple train passes, were measured. The vibration levels remained low under all conditions, demonstrating that this particular type of GFRP bridge is suitable for railway crossings and that further optimisations may be available to designers while meeting vibration serviceability limits. However, consideration of the loadings suggests GFRP bridges may be more susceptible to higher pedestrian harmonics than traditional structures, and that vibrations from train buffeting are likely to be a design consideration for future bridges over high speed lines.

1. Introduction

Glass Fibre Reinforced Polymer (GFRP) composites are an increasingly attractive construction material when it comes to building pedestrian bridges over railway lines. The lightweight nature of GFRP footbridges contributes to quick installation with minimum impact on the railway traffic and line closures. Good durability and low maintenance requirements are additional benefits that are reflected in rare disruptions over the lifetime of the structure. Additionally, the high strength-to-weight ratio makes them ideal for the typical spans required across tracks [1], around 12–20 m. However, due to the low density and relatively low stiffness compared to traditional materials, GFRP bridges could potentially suffer excessive vibrations when exposed to dynamic loading [2]. Such serviceability issues are increasingly found to govern the design of GFRP structures [3,4].

The potential for excessive vibrations of lightweight structures due to human induced loading is a well-known issue that requires special consideration [5,6]. It is important to obtain experimental insight into the behaviour of existing GFRP bridges as there is currently a lack of experimental data on the dynamic characteristics and performance of this type of structure. Additionally, further advice on the suitability of existing generic guidelines for the vibration serviceability limit state (VSLS) due to human induced dynamic loading on GFRP footbridges is required. One of most popular guidelines, Setra [7], implies that footbridges with fundamental natural frequencies above 5 Hz and 2.5 Hz for vertical and lateral vibration modes, respectively, automatically satisfy VSLS requirements and therefore do not require calculation of the vibration response. The UK National Annex to Eurocode 1 [8] sets the limit for the vertical direction to 8 Hz and about 1.7 Hz for lateral modes. These two guidelines cover excitation frequencies up to the third harmonic of the dynamic force by walking in the vertical direction and up to the second harmonic in the lateral direction, which contain most of the excitation energy. They, therefore, imply that the frequency content of the human induced dynamic force above these cut-off values is not strong enough to excite the structure. This guidance is known to be adequate for most footbridges made of traditional materials but might be inappropriate for lighter, and generally easier to excite, structures. Interestingly, the International Organization for

* Corresponding author.
E-mail address: j.russell.3@warwick.ac.uk (J.M. Russell).

https://doi.org/10.1016/j.engstruct.2020.110756
Received 21 June 2019; Received in revised form 6 April 2020; Accepted 5 May 2020

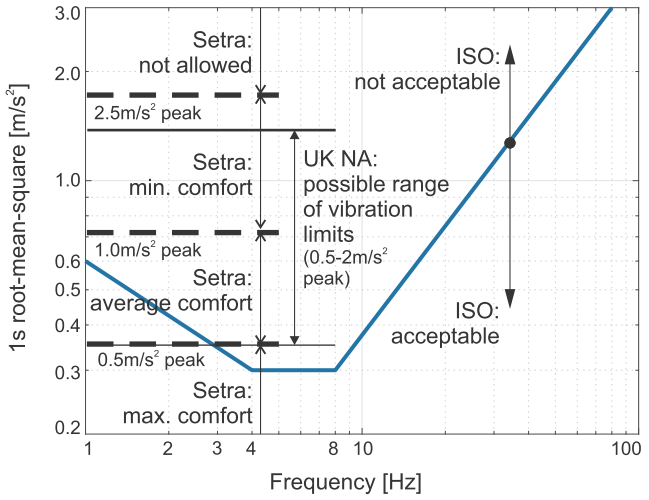

Fig. 1. 1s RMS vibration limits for a pedestrian by three design guidelines. Both axes are shown in log scale.

Standardization (ISO) guideline [9] is more cautious. Its model of the walking-induced force includes the first five harmonics. Given that walking activity is typically in the frequency range 1.4–2.5 Hz [5], the ISO extends the frequency range of interest on footbridges to about 12 Hz (in the vertical direction). As it includes a wider frequency range of the excitation force, the ISO model currently seems to be the best available candidate for evaluation of VSLS for GFRP structures. The vibration limit defined in ISO is also the most comprehensive as it accounts for differences in human response to vibration at different frequencies (up to 80 Hz), while the [7,8] limits are independent from vibration frequency and only meant to be used for low frequency structures. The vibration limits (in 1s root mean square (RMS) equivalent) for a walker exposed to vibration in the vertical direction, as defined by the three guidelines, are shown in Fig. 1. It should be noted that the ISO guidance relevant for VSLS under human loading is presented in informative (rather than normative) annexes. This is, most likely, due to awareness that human loading and vibration response are complex to model, and therefore not every relevant loading case can be considered and evaluated adequately by the proposed method for every possible structure.

Contrary to narrow-band human induced dynamic loading, a running train is a source of multiple broad-band vibrations that radiate into its surroundings. These include effects caused by engine noise, the interaction between train wheels and track and periodic loading due to sleeper spacing or based on the distance between axles or wheel groups [10]. Such vibrations may be transferred to the bridge via the track and foundations. These excitation sources are dependent on the train speed and typically act at higher frequencies than is a concern for many footbridges, however, conditions can allow lower frequency events as well. In addition, a pressure wave due to a train passing beneath a structure creates an aerodynamic buffeting effect on the bridge described by a positive pressure peak immediately followed by suction at the head of the train [11]. To date, little attention has been given to the dynamic characteristics of the time-pressure history, but it is likely to be dominated by responses well below 10 Hz, and increasing with train speed. Although much work has considered the effect of railway induced vibrations from high speed trains as they travel on bridges [12,13], there exist only limited investigations into the response of GFRP bridges located over railway lines [14–16]. These have highlighted the concern designers have in using lightweight materials, like GFRPs, in such locations, and the difficulty in predicting vibration responses due to train buffeting.

While recent work, such as Drygala et al. [4], has applied current guidelines to numerical models of theoretical GFRP structures, including human and train induced vibration, there is still a lack of experimental data to validate both structural and loading models. This paper investigates the vibration response of a 14.5 m GFRP truss footbridge over a railway line. The modal properties of the structure were determined from impact hammer testing followed by experimental investigations of pedestrian and train induced vibration. Further analysis was then performed to evaluate the bridge response to human and passing train dynamic loading and critically evaluate the suitability of some existing design guidance and recommend improvements.

2. Bridge details

Dover Seawall Wellards Way consists of two separate, simply supported, 14.5 m GFRP truss footbridges, on top of concrete piers (Fig. 2), one of which is over two railway tracks. The bridge, installed in January 2017, is located in the south east of England providing pedestrian access to the nearby beach. The train line is part of the Dover to Folkstone

(a) Photograph of the bridge

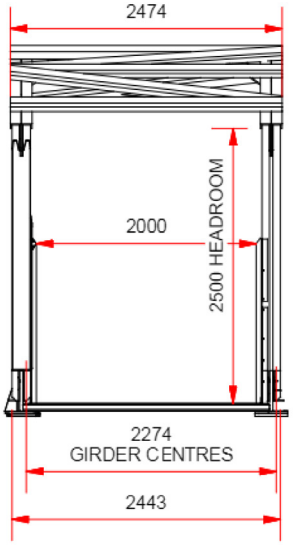

(b) Cross section

Fig. 2. Dover Seawall Bridge.

route operated by Southeastern. It was designed and built by Pipex px® to replace an older bridge after the section of railway was damaged by flooding. The bridge was constructed with pultruded and infused glass FRP sections, bolted and bonded into a 3.325 m high truss. The primary truss members were pultruded 203x9.53 EXTREN® channel sections, placed back-to-back with a 30 mm gap, separated by a plate bonded to the flanges. Larger, 254x12.7 EXTREN® channel sections were used at the ends of the span. These EXTREN® sections have a quoted longitudinal modulus of 17.2GPa [17]. The top chord was an infused T-shape glass FRP section, moulded to give a camber of 585 mm at the middle. Typically 5 or 6 bolts were provided to connect the channel sections to the top chord or the deck. The 2.4 m wide deck was resin infused FRP, between 5 and 14 mm thick, with a T90.210 foam core to give a maximum deck thickness of 72 mm and provides a flat walking area 2 m wide. A 3 mm infused floor plate was also included. Cross bracing using GFRP sections at the top increases the lateral stiffness of the bridge. The 1.5 m high GFRP parapet panels were designed as a modular system and bolted to the truss members allowing for bolt inspection at the nodes. The bridge sits on 6 m high concrete piers to provide clearance over the railway track and utilises a pinned bearing support at one end and a roller bearing at the other. These bearings are made of 316 stainless steel and sit on natural rubber bearing pads with chemical anchors directly into the concrete piers. The roller bearing is generated by using PTFE in between the rubber pad and the steel or concrete. The pads provide better load distribution locally, and also add some dampening. The total mass of each span is 5.5 tonnes.

3. Modal analysis

After the bridge was completed it underwent quality control testing in Pipex's factory. This included checking of the modal properties, conducted by the University of Warwick in November 2016. Once the bridge was installed on site its dynamic characteristics were retested in January 2017. This allowed any potential changes to the modal properties to be identified, and consideration given to the suitability of factory quality control tests for predicting responses for vibration serviceability limit state design criteria.

3.1. Modal testing at the factory and on site

Impact hammer testing was initially carried out on one of the Dover Seawall Bridge spans while it was in the factory to identify both lateral and vertical vibration modes. The structure was complete, with the exception of the final floor plate that had not been installed due to time constraints. The bridge's supports were set up with the intention to match the designed boundary conditions once in service. Seven Honeywell QA750 accelerometers (nominal sensitivity of 1300 mV/g) and an instrumented sledge hammer (Dytran Model 5803A, sensitivity 0.23 mV/N) were used for the tests. To identify the first few vibration modes of the bridge a grid of fourteen measurement points on the deck was utilised (Fig. 3) by employing a roving accelerometer method. The test point (TP) 3, at which the modes of interest were observable, was chosen as the impact location. Vertical impacts were applied to the deck and lateral impacts to the base of the diagonal truss member. Vertical and lateral vibrations at the 14 TPs due to vertical and lateral impacting at TP3, respectively, were measured, resulting in 28 frequency response functions (FRFs) to be acquired. Since only seven accelerometers were available, the test campaign was divided into two setups for each direction. The impulse force signal was the reference linking different setups. The eight signals in each setup were recorded simultaneously using a 16 channel data logger by Data Physics (SignalCalc Mobilyzer).

A sampling frequency of 1024 Hz and an 8s capture window were used. A rectangular window of length 240 ms was applied to the force channel to remove the noise that might be present on the excitation signal (typical force duration was around 10 ms). An exponential window was applied to all channels to reduce the effects of leakage. The additional damping introduced in this way was corrected for in the later analysis [18]. To further reduce the effects of measurement noise, an average of eight measured FRFs was calculated.

A similar method of modal testing was applied on site. This time, however, only three Honeywell QA750s accelerometers were utilised due to use of a smaller four channel Data Physics Quattro logger and no window was applied to the response signals on site due to their fast decay.

3.2. Measured modal properties

Vertical flexural and torsional modes were identified by curve fitting the FRFs calculated from measured vertical acceleration responses and the corresponding vertical impact force. Lateral modes were identified separately by curve fitting the FRFs related to the lateral acceleration response from lateral impacts.

More specifically, a global Rational Fraction Polynomial method [19,20] integrated in ME scope 6.0 software [21] was used for the curve fitting of FRFs to estimate the modal properties (i.e. natural frequencies, damping ratios and mode shapes) of the bridge. For the sake of completeness, the theory for modal analysis using data from impact hammer tests is briefly introduced here.

FRFs can be represented either in rational fraction form or partial fraction form, which are equivalent to each other. The partial fraction expansion of FRF matrix may be written as

$$[H(\omega)] = \sum_{k=1}^{n} \frac{[R_k]}{j\omega - p_k} + \frac{[R_k^*]}{j\omega - p_k^*} \tag{1}$$

where $[H(\omega)]$ is the $n \times n$ FRF matrix. $p_k = -\zeta_k \omega_k + j\omega_k \sqrt{1-\zeta_k^2}$ is the pole for the k-th mode. ω is the frequency variable. ζ_k, ω_k and $[R_k]$ are the damping ratio, undamped frequency and the matrix of residue (i.e. mode shape component) for the k-th mode, respectively, which are the unknown parameters to be identified in parametric model given by Eq.

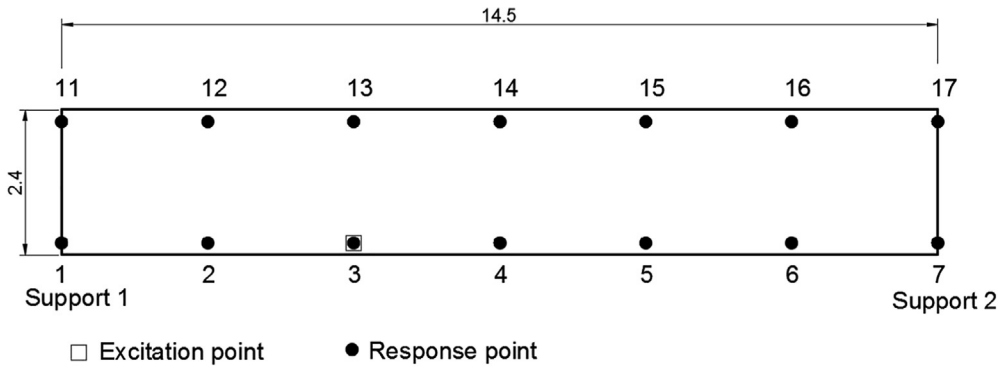

Fig. 3. Test grid.

Table 1
Measured vibration modes.

Description	Frequency (Hz)		Damping (%)	
	Factory	Site	Factory	Site
Lateral	/	3.6	/	0.8
Lateral	4.1	/	0.9	/
Lateral	/	4.3	/	1.1
Lateral	/	6.0	/	0.8
Lateral	/	9.8	/	1.5
Lateral	14.4	14.0	2.0	1.6
Lateral	15.7	/	2.1	/
Vertical	16.6	15.1	0.9	1.4
Vertical	/	16.7	/	1.4
Lateral	/	16.9	/	1.2
Torsion	20.7	20.0	1.7	0.2
Torsion	22.0	22.5	0.8	1.3
Torsion	23.5	/	1.4	/
Vertical	28.8	26.9	1.4	2.0

1.

In the Rational Fraction Polynomial method, FRFs are first expressed as the ratios of two polynomials. They are then curve fitted to measured FRF data such that the coefficients of numerator and denominator polynomials are identified. Next, the identified rational fraction parametric models of FRFs are rewritten into their partial fraction expansion counterparts, and the frequency, damping ratio and mode shape for each mode of interest are then estimated.

The modes up to 30 Hz were identified and are summarised in Table 1. Key lateral and vertical modes are shown in Fig. 4. The main difference in the site and factory results is the appearance of additional low frequency lateral modes in the site testing. On site there are four lateral modes up to 10 Hz while only one from the factory condition. This is due to the final bridge being a two-span truss structure with a common centre pier whereas the factory test was done on bearing pads and rigid blocks sitting directly onto the concrete floor. The additional modes are therefore part of global modes of the whole structure, including the support pier. Fig. 4(a) and (b) give insight into the movement of the supports demonstrating the different mode shapes for this span. The first symmetrical lateral mode was identified at 14.4 and 14.0 Hz for the factory and site, respectively (Fig. 4(c)). The first vertical flexural mode was at a frequency of 15.1 Hz on site and corresponds to the 16.6 Hz mode in the factory. The difference is due to movement of the supports that appears in site tests (Fig. 4(d)). There is also another vertical mode that was detected on site at 16.7 Hz which involved asymmetric movement of the supports and a torsional component. The first torsional mode was at a frequency 20.7 Hz (factory) and 20.0 Hz (site).

This study shows that the modes which appear in both site and factory testing have similar natural frequencies and mode shapes. The appearance of additional modes in site conditions, however, demonstrates that conducting only a test in a factory is unlikely to fully replicate all aspects of the dynamic behaviour of the structure. In this case it is due to the existence of the concrete piers and finishes (such as the floor plate) on site that affect the mass and the stiffness of the bridge to some degree. Therefore, testing the structure in as-built conditions is the most reliable means of evaluating the actual dynamic behaviour, whilst the pre-installation tests should be used for identification of potential major issues with the behaviour of the superstructure.

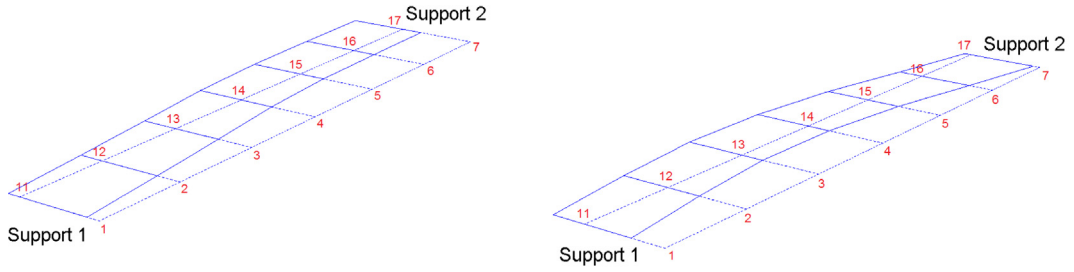

(a) Lateral mode involving movement of support 2 at 3.6Hz

(b) Lateral mode involving movement of support 1 at 4.3Hz

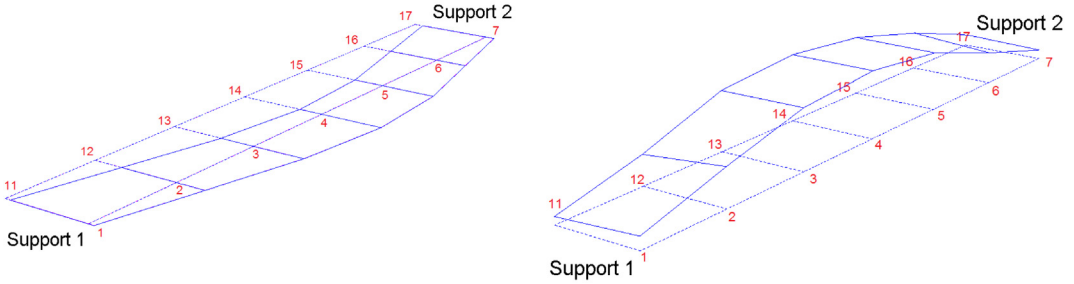

(c) Lateral flexural mode at 14.0Hz

(d) Vertical flexural mode at 15.1Hz

Fig. 4. Example mode shapes from on site testing. Support locations and TPs are also shown.

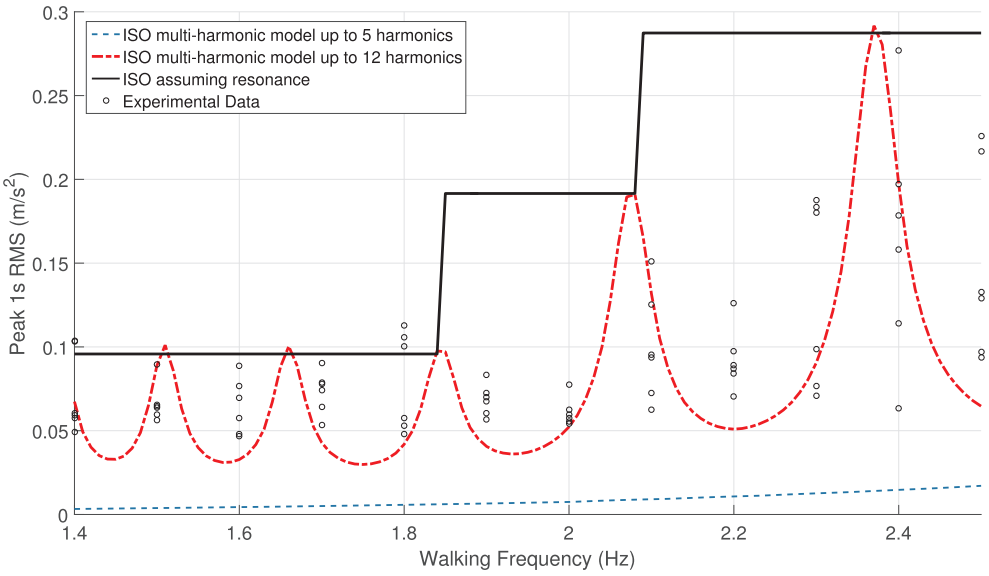

Fig. 5. Mid-span acceleration response from single pedestrian walking (1.4–2.5 Hz).

Natural frequencies for this bridge (at and above 3.6 Hz for lateral and 15.1 Hz for vertical modes) are well above the values considered potentially problematic according to [7], UK NA [8] and even [9] guidelines, and therefore these guidelines would not require vibration serviceability checks. Whether this conclusion is suitable for this bridge and similar GFRP structures will be analysed by utilising the ISO method and critically evaluating its performance against experimental and numerical data. Furthermore, as train buffeting effects are expected to be more critical for lower frequency modes (say below 10 Hz), the appearance of four lateral modes on site requires consideration of this loading case.

4. Human induced vibration

Tests involving multiple human induced loading scenarios were conducted in the factory to investigate the effects on the bridge and the ability of the ISO guidelines to predict the measured responses. The peak 1 s root-mean-square (RMS) acceleration limits for this bridge are 0.57 m/s^2 (at frequency of 15.1 Hz; site condition) and 0.62 m/s^2 (at frequency of 16.6 Hz; factory condition) in the vertical direction (Fig. 1) and about 1.6 m/s^2 for vibration frequency of about 14 Hz in the horizontal lateral direction (ISO, 2007). Note that frequencies below 10 Hz made negligible contribution to the lateral response, which was the reason for their exclusion from the analysis. The tests under human (single pedestrian and crowd) excitations were initially conducted with the aim to identify potential vulnerability to human actions and to inform tests on site. Namely, crowd tests would only be organised on site if they can add significant value to understanding in-service performance. This also helps demonstrate that for a potential human induced vibration concern, the in-factory condition provides useful information for VSLS.

4.1. Single pedestrian walking

ISO guidelines define the dynamic vertical force in the time domain F_v for a walking human with Eq. 2 [9]:

$$F_v(t) = Q \sum_{n=1}^{k} \alpha_{n,v} \sin(2\pi n f t + \phi_{n,v}) \tag{2}$$

where Q is the pedestrian's static weight, f is the pacing frequency, n is the integer harmonic and k is the number of harmonics of interest. $\phi_{n,v}$ is the phase angle of the nth harmonic, taken conservatively as 90° for contributions below resonance. These guidelines only define the amplitudes of the pedestrian induced dynamic force, $\alpha_{n,v}$, up to the 5th harmonic as a percentage of their weight, assuming an average pedestrian weighs 700 N. The first harmonic is defined as function of pacing rate (typically between 100–360 N for usual walking frequencies). The second is taken as 10% of the pedestrian weight (70 N) and a value of 6% of the weight (42 N) for 3rd-5th harmonics. This implies that maximum frequency for which resonance might occur would be about 12 Hz, i.e. structures above this value do not have vibration issues due to walkers.

To determine if this approach is suitable for representing the vibration response of this case structure, a modal model of the Dover Seawall bridge was developed in MATLAB [22]. Within this method the bridge was represented as an equivalent single degree of freedom (SDOF) model corresponding to the first vertical mode. The modal stiffness and damping coefficients, k_b and c_b, of the bridge are determined from the known natural frequency and damping ratio identified in the factory tests (see Table 1). The modal mass, m_b, is estimated to be 2672 kg using the approach given in [23], integrated in the commercial software MEscope 6.0 [21]. The second-order differential equation of modal displacement, y, with respect to time, Eq. 3, can then be formed:

$$m_b\ddot{y}(t) + c_b\dot{y}(t) + k_b y(t) = F_v(t)\Phi(vt) \tag{3}$$

where the right hand side is the vertical force waveform of a pedestrian in the time domain, $F_v(t)$, weighted by the first mode shape ordinate at the position of the walker, assumed to move over the bridge with constant speed, v. The measured spacial function of the vertical mode shape, $\Phi(x)$, was transformed to the time domain via $x = vt$.

A VSLS assessment was made by applying the ISO's five harmonic forcing model (Eq. 2) and solving Eq. 3 using the fourth-order Runge-Kutta method. Typical walking speed of 1.7 m/s [8] and a range of pacing rates were simulated to obtain the modal accelerations. The calculated modal response represents the contribution of the first mode to the physical acceleration at the mid-span. Use of the experimental modal model is useful for accurate analysis of VSLS as it only uses parameters determined experimentally, and therefore avoids introducing additional uncertainties (such as exact knowledge of boundary conditions) in the response analysis, which would be the case if a finite element model was utilised.

The calculated peak 1s RMS acceleration response is shown as a dashed line in Fig. 5. The resulting low vibration level is certain to underestimate the actual response of the bridge as the frequency

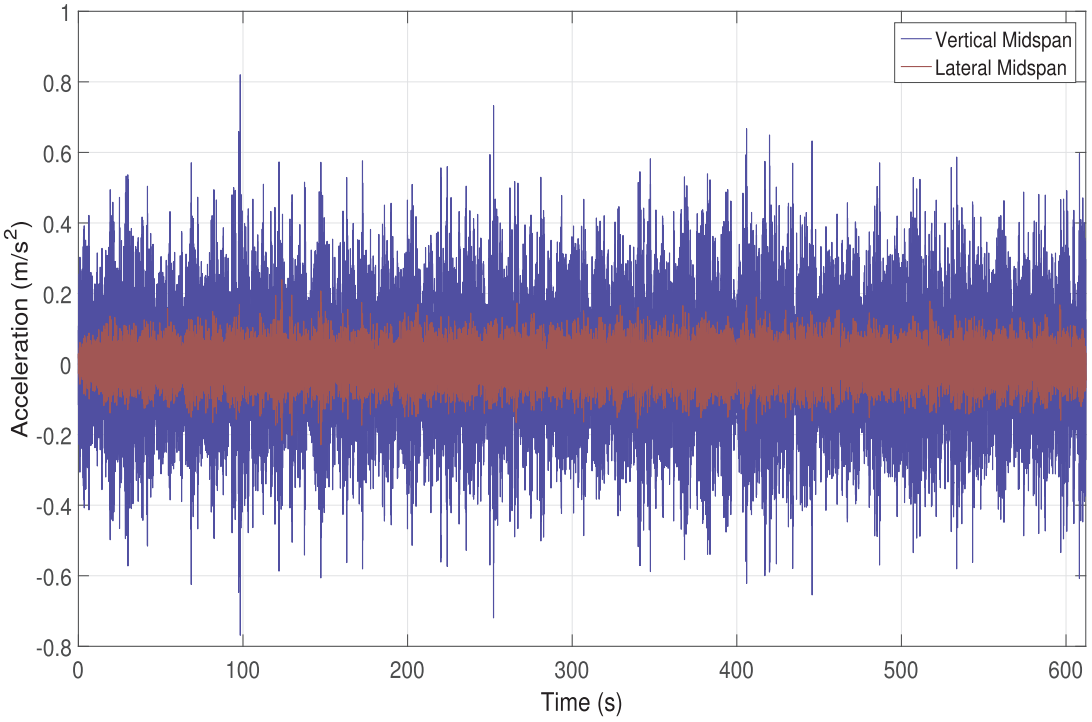

(a) Mid-span acceleration responses to a pedestrian crowd of 15 people

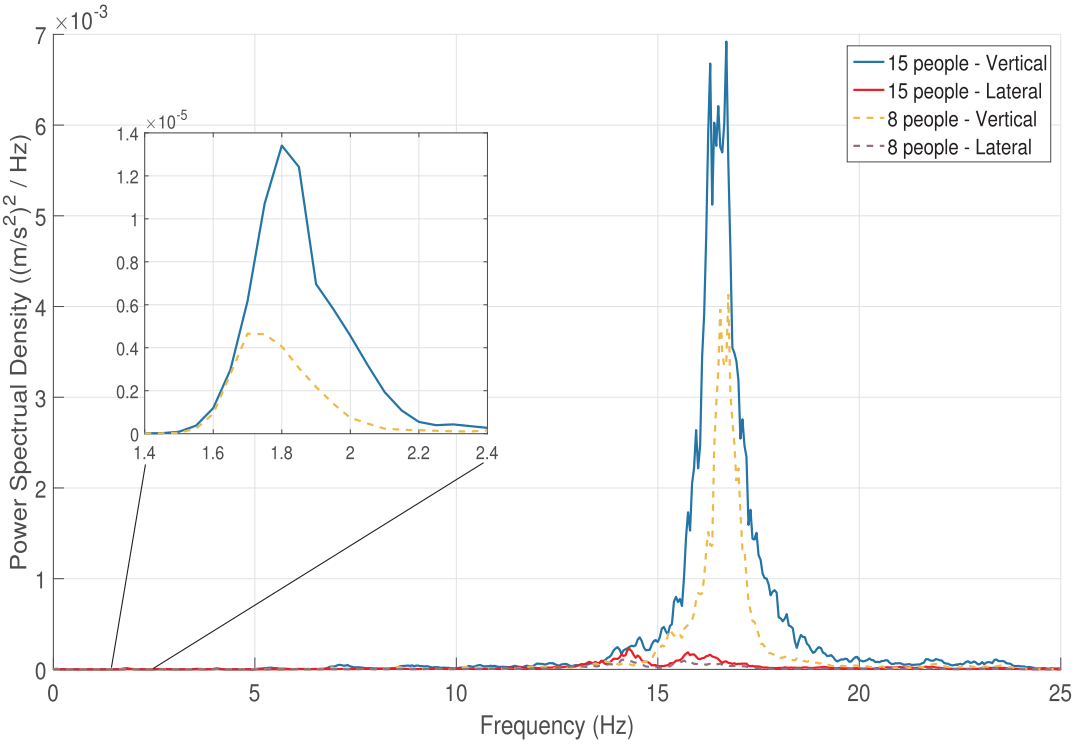

(b) PSD of the acceleration data from crowd loading

Fig. 6. Responses to pedestrian crowd loadings.

content of the loading model is not able to excite a bridge with a fundamental natural frequency of 16.6 Hz.

To determine the actual response, three test subjects (TSs) took part in "single person walking" tests in the factory. Each walker initially crossed the bridge at a set, metronome-controlled, pacing rate of 1.4 Hz and then waited for the vibrations to die down before making a return crossing at the same frequency. Once the bridge was at rest again the walking frequency was increased by 0.1 Hz and the test continued until a pacing frequency of 2.5 Hz was reached. The aim was to expose the bridge to the full range of possible pacing frequencies. The vertical

acceleration records at the midpan (TP4 in Fig. 3) were low-pass filtered at 20 Hz to remove high frequency noise caused by factory machinery and the response from higher modes. The peak 1s RMS results from all cases are given as circles in Fig. 5. It can be seen that these measured responses are an order of magnitude larger than the ISO model predicted. The vibrations reached up to 0.28 m/s^2 for walking at 2.4 Hz. The maximum response is caused by the natural frequency of the bridge being close to the 7th walking harmonic. This example suggests that higher harmonics above the 5th have enough energy to excite this lightweight structure. To improve the ISO model, an extended ISO model which accommodates up to 12 harmonics is proposed here. To reflect the fact that the energy of higher harmonics decreases, a value of 3% of the person's weight was taken for harmonics six and seven, 2% for the 8th and 1% for harmonics 9–12. These values are based on the authors experience with research in pedestrian induced dynamic loading. The numerical values for these harmonics are not readily available in the literature, since they are not required in vibration checks of bridges made from traditional construction materials.

The dash-dotted line in Fig. 5 shows the result of this extended multi-harmonic model. It demonstrates that the predicted vibration response is much more in line with the experimental data. The peaks show the walking frequencies that corresponds to sub-multiples of the natural frequency. The experimental data does not match this model exactly in terms of identifying the most effective pacing rates due to uncertainties in the TSs walking at exactly the correct frequency and the broadening of the excitation peaks at higher harmonics which the ISO model does not account for.

To have a conservative estimate of the response (usually preferred in design practice), an envelope of the previous results could be drawn (solid line in Fig. 5). This is equivalent to assuming that a pedestrian walks to excite a resonance response. Namely, the response for walking at frequencies 1.40 to 1.84 Hz is estimated assuming the 9th harmonic of walking at 1.84 Hz excites the resonance at 16.6 Hz, for walking at 1.85 to 2.08 Hz, it is assumed that the 8th harmonic for walking at 2.08 Hz causes the resonance. For walking at 2.05–2.5 Hz, resonance by the 7th harmonic is achieved by walking at 2.37 Hz. This response envelope covers the observed results well, as shown in Fig. 5.

The peak 1s RMS acceleration vertical response in single pedestrian test was 0.28 m/s^2, which is less than the ISO limit of 0.62 m/s^2 for this bridge, suggesting that vertical vibrations due to individual walks are not a concern. The peak 1s RMS lateral response was only 0.029 m/s^2, i.e. well below the limit of 1.6 m/s^2, which was the reason not to analyse it in this paper, as stated previously.

4.2. Crowd loading

To get an insight into the VSLS of the bridge to multi-person traffic, crowd loading scenarios were tested. A group of eight and a group of 15 people walked continually across the bridge in a circular system for about 11 min. When a person reaches the end of the bridge they walk off, turn around and then step on again, returning along the bridge. This resulted in two continuous lines of traffic characterised by crowd densities of about 0.2 and 0.4 pedestrians/m^2, respectively. The mass of the occupants is estimated to be around 1150 kg for the larger crowd case and about 610 kg for crowd of 8 people. The traffic density of 0.2 pedestrians/m^2 corresponds to a spatially unrestricted traffic scenario in which people have enough space to overtake and not be influenced by their neighbours. The 0.4 pedestrians/m^2 density represents a scenario where pedestrians might occasionally need to adapt to the actions of their neighbours in terms of speed of walking and to find space for overtaking [24]. In both scenarios the walkers were free to pick and vary their own comfortable walking speeds based on their surroundings.

Fig. 6(a) shows the vertical and lateral acceleration signals recorded at the mid-span during the larger crowd test. A low-pass filter, set at 20 Hz was applied. Peak accelerations of 0.82 and 0.24 m/s^2 occurred for the vertical and lateral directions, respectively. An averaged Fourier Transform was taken of 20s long segments of the signal, with an overlap of 50%. A Hanning window was applied to reduce energy leakage. Fig. 6(b) shows the power spectral density (PSD) of the two signals. The first vertical mode at 16.6 Hz is clearly excited most, as is a lateral mode at around 14.4 Hz, in line with previous observations about excitability of the modes on this bridge. It is interesting to mention that a close look in the frequency content of the spectrum in the 1.4–2.4 Hz range reveals that the average pacing frequency of the crowds was about 1.8 Hz and 1.7 Hz for 15 and eight people, respectively. This can be seen in the enlarged detail in Fig. 6(b).

The larger crowd produces larger vibrations, as expected, with a vertical peak 1s RMS of 0.35 m/s^2. The smaller crowd of eight had a peak 1s RMS of 0.24 m/s^2. Therefore, even under crowd loading, this bridge is not expected to attract adverse comments from its users. In addition, none of the participants reported any concern in relation to vibrations perceived during the tests. This outcome of the tests in the factory influenced the decision that site testing should concentrate on modal testing and train buffeting effects only.

To check the ability of the extended ISO model to replicate these crowd loading events, a set of simulations was performed. A group of 15 pedestrians was generated by setting their initial position on the bridge deck 2s apart. Each person's force was then represented by 12 harmonics. It was assumed that each pedestrian has a static weight of 750 N (to reflect the actual crowd that took part in the tests) but a randomly assigned walking frequency and step length. The pacing frequency was drawn randomly from a normal distribution having a mean value of 1.8 Hz, as seen in the experiments, and standard deviation of 0.19 Hz [25]. Similarly, step length was assumed to follow a normal distribution having mean value of 0.75 m and standard deviation of 0.08 m [25]. The pedestrians were assumed to walk along a circular route equivalent to that used in experiments. Each pedestrian walked at a different speed that was calculated by multiplying the step length and pacing frequency. A time history of the dynamic force was then created by scaling each pedestrian's walking force to the first mode shape and superposing the forces by all the pedestrians. This resulting force was then applied to the modal model of the bridge used previously (see Eq. 3) to obtain the acceleration response. The peak 1s RMS value was calculated from a 400s response time, ignoring the starting period while the bridge response was building up. The simulation was then repeated 100 times and the average peak 1s RMS value taken. Simulations were then conducted in the same way for a group of eight people, with a mean pacing frequency of 1.7 Hz. The model predicts a value of 0.38 m/s^2 for the crowd of 15 and 0.25 m/s^2 for eight people. These values are in excellent agreement with the measured results. They demonstrate that the proposed extension of the ISO model can be used for modelling crowds.

4.3. Parametric study

All the vibration responses for this bridge have been within the ISO limit and this seems to justify not requiring VSLS check for this bridge with a natural frequency as high as 16.6 Hz. However, this conclusion raises an interesting question as to if this is always the case or if there are other similar span GFRP bridges for which the ISO limit might be exceeded.

To provide answer to this question, a parametric study is performed here. This bridge has mass per unit area of about 158 kg/m^2. This low value is similar to the mass of other GFRP bridges, although even lower masses are possible. For example a girder GFRP bridge spanning 14.7 m has a mass of about 100 kg/m^2, and it results in a lower natural frequency of 6.9 Hz [26] due to the lower stiffness of the girder system. To consider the influence of dynamic characteristics on the response, a series of representative structures were modelled by assuming a theoretical case of a bridge with a similar properties as the case study, i.e. mass of 150 kg/m^2, deck width of 2.4 m, span of 15 m, a damping ratio

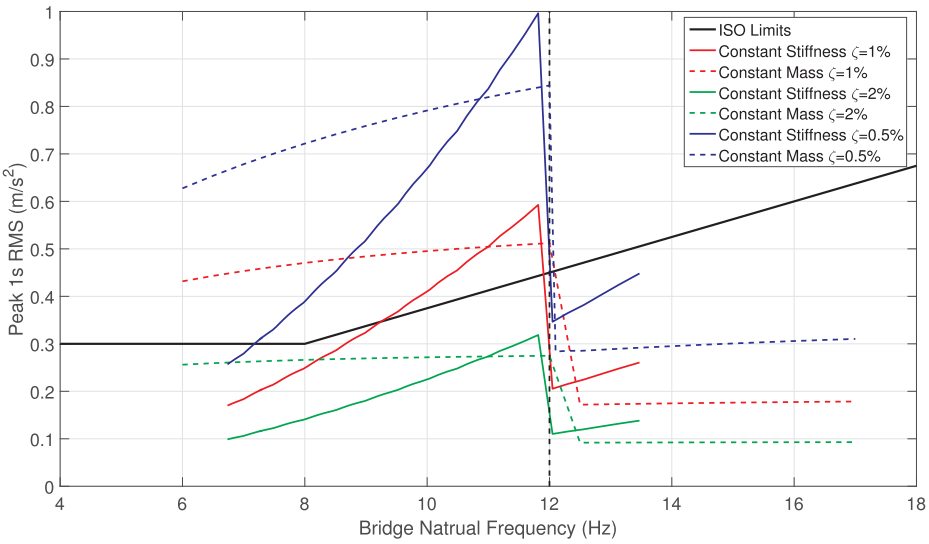

(a) Single pedestrian

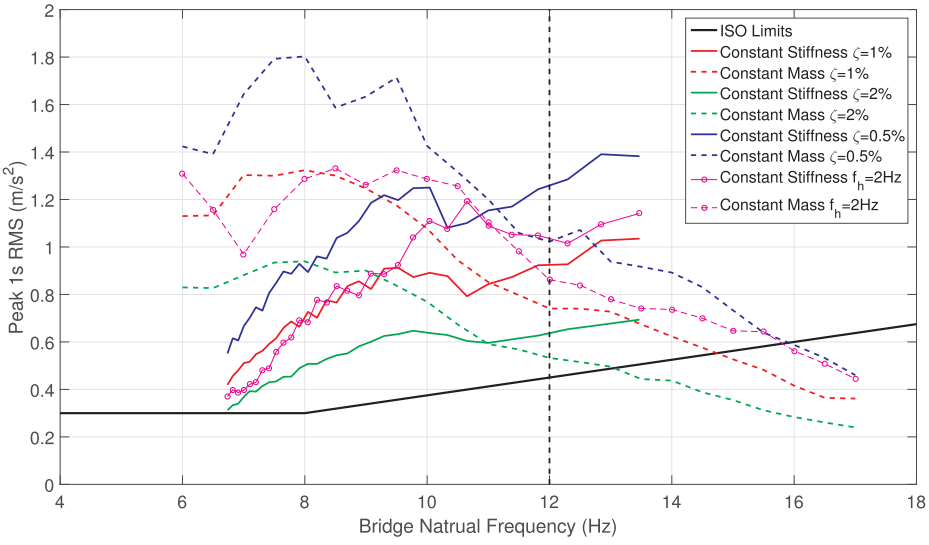

(b) Crowd of pedestrians

Fig. 7. Peak accelerations from parametric study of bridge configurations. ISO limits are also shown.

of 1.0% and a half-sine mode shape. However, the natural frequency was varied (by appropriately reducing the stiffness) from 17 Hz down to 6 Hz to consider the range likely for such structures, regardless of their structural configuration or other design properties. The acceleration response to a pedestrian walking at a speed of 1.7 m/s and generating the force as per Eq. 2 was calculated by solving Eq. 3, assuming resonance in one of the higher harmonics. The peak 1s RMS acceleration response ("Constant mass, $\zeta = 1\%$") is shown as a function of the bridge frequency in Fig. 7(a). These results demonstrate that bridges with frequency below 12 Hz have a potential to suffer from excessive vibrations.

In another set of simulations, the stiffness of the bridge is taken to be equal to the stiffness of the 11 Hz bridge from the previous example (that is bridge in the middle of the frequency range previously considered), and the mass is varied in a feasible 100–400 kg/m^2 range. In this case the response ("Constant stiffness, $\zeta = 1\%$") exceed the limit when the natural frequency is between 9.3 and 12 Hz. Additionally, bridges with other damping ratios of 2% and 0.5% are also presented. As expected the lower damping ratio results in larger vibrations with more configurations exceeding the ISO limit. Finally, it can be seen that no case presented here exceeded the ISO limit if the natural frequency of the bridge is above the 12 Hz value assumed by the ISO model (shown as a vertical dashed line). This is due to the much lower energy associated with harmonics above the 5th and their difficulty in exciting resonance. However, the analysis also shows that the Setra and UK NA to Eurocode 1 approach of not requiring VSLS analysis if the bridge has a fundamental natural frequency above 5 Hz and 8 Hz, respectively, is not necessarily applicable to bridges made of GFRP composites. Further consideration may also be required for higher energy single pedestrian events such as running or jumping.

The parametric study was repeated for a crowd of 15 people. A multi-harmonic forcing model was used for each pedestrian. Individual pacing frequency was sampled from a normal distribution with a mean frequency of 1.8 Hz, as before. Fig. 7(b) shows the peak 1s RMS values. The results (solid and dashed lines in the figure) suggest that VSLS is not satisfied in the majority of cases, not even in many instances when

Table 2
Train information.

Train ID	Train Type	Direction	Speed			Error
		(from)	(m/s)	(mph)	(km/h)	(m/s)
375-D-1	375	Dover	19.1	42.6	68.6	0.13
375-D-2	375	Dover	19.5	43.6	70.1	0.13
375-D-3	375	Dover	18.5	41.3	66.5	0.12
375-D-4	375	Dover	19.8	44.3	71.3	0.14
375-D-5	375	Dover	18.8	42.2	67.8	0.13
375-D-6	375	Dover	17.1	38.3	61.6	0.11
375-F-1	375	Folkstone	21.4	47.9	77.0	0.32
375-F-2	375	Folkstone	19.6	43.9	70.6	0.13
375-F-3	375	Folkstone	14.9	33.3	53.6	0.13
375-F-4	375	Folkstone	19.1	42.7	68.8	0.13
395-D-1	395	Dover	19.6	43.8	70.5	0.16
395-D-2	395	Dover	16.8	37.6	60.5	0.12
395-D-3	395	Dover	19.8	44.4	71.4	0.16
395-D-4	395	Dover	20.0	44.7	71.9	0.16
395-D-5	395	Dover	19.7	44.1	70.9	0.16
395-F-1	395	Folkstone	18.6	41.5	66.8	0.15
395-F-2	395	Folkstone	20.0	44.8	72.1	0.22
395-F-3	395	Folkstone	21.7	48.6	78.3	0.19
Freight-F-1	73/9	Folkstone	10.7	23.9	38.4	0.19

the natural frequency of the bridge is above 12 Hz. Finally, a case with a faster crowd was also considered, taking an average pacing frequency of 2 Hz and a damping ratio of 1%. This increases the vibration levels (see the lines with circle markers in Fig. 7(b)) particularly for bridges with higher natural frequencies, as resonance effects can be achieved with lower order (i.e. stronger amplitude) forcing harmonics.

The parametric study provides an important insight into the possible range of vibration responses for different (and realistic) combinations of system parameters. It shows that neither the existing frequency limits nor loading models that include five harmonics only are directly applicable to VSLS assessment of GFRP footbridges.

5. Train-induced excitation

Before the bridge was opened to the public, it was instrumented and monitored for multiple types of train passes that would be typical for its service life. Data from 19 trains were recorded in the afternoons of two week days in January 2017, between 12:00 and 17:00. Site conditions, including low visibility due to fog and nearby construction work, meant that not every train was able to be logged. In order to consider the potential issue of train buffeting pressure sensors were installed on the soffit and parapets of the bridge and four accelerometers were placed to measure vertical response at the mid-span and supports (i.e. TP1, 4 and 7 in Fig. 3) and the lateral response at TP4. Differential pressure sensors (TiTec DDMx/2, ±20 mbar) were used, with one port connected to be perpendicular to the external face, and the other connected to a common sealed reference box. Consideration of the pressure measurements allows identification of the moment of the positive peak at the head of the train, and the symmetrical response at the end. These results help provide insight into the cause and extent of excitation possible for such a structure.

5.1. Train information

Although the bridge was designed for a train line speed of 75mph (120 km/h), nearby track restrictions heavily limited the speed that trains can achieve on this section of rail. Table 2 provides information on 19 trains that passed under the bridge during the observed period. Trains travelling from Dover are called D in the table while those from Folkstone are identified as F. The two common types of train were a British Rail Class 395 'Javelin' and the Class 375 'Electrostar' travelling between 30-50mph (50–80 km/h) while passing the bridge. The Class 395 has a streamlined nose designed for high speed lines, while the 375 has a flat front face. Additionally there was a slow moving (24mph, i.e. 38 km/h) Class 73/9 rail freight train as well. The speed of the trains was estimated using the passing time from video footage and the known length of the coaches [10]. The stated speed errors in Table 2 are due to estimations on train carriage lengths and the frame rate of the camera.

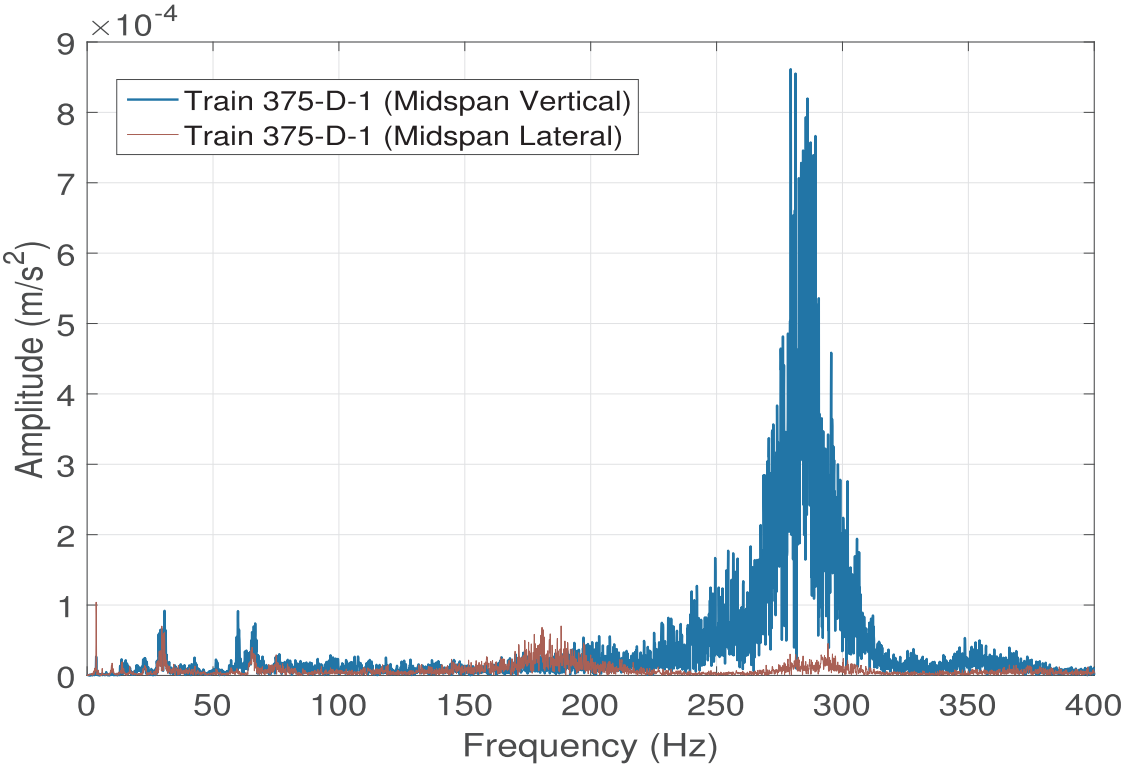

Fig. 8. Frequency spectrum from a typical train pass.

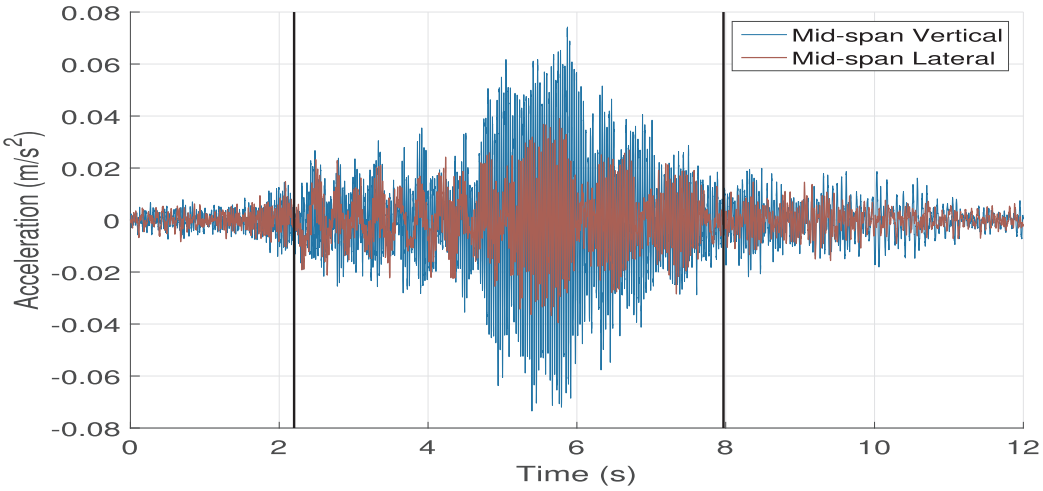

(a) Train 395-F-3 (21.7m/s)

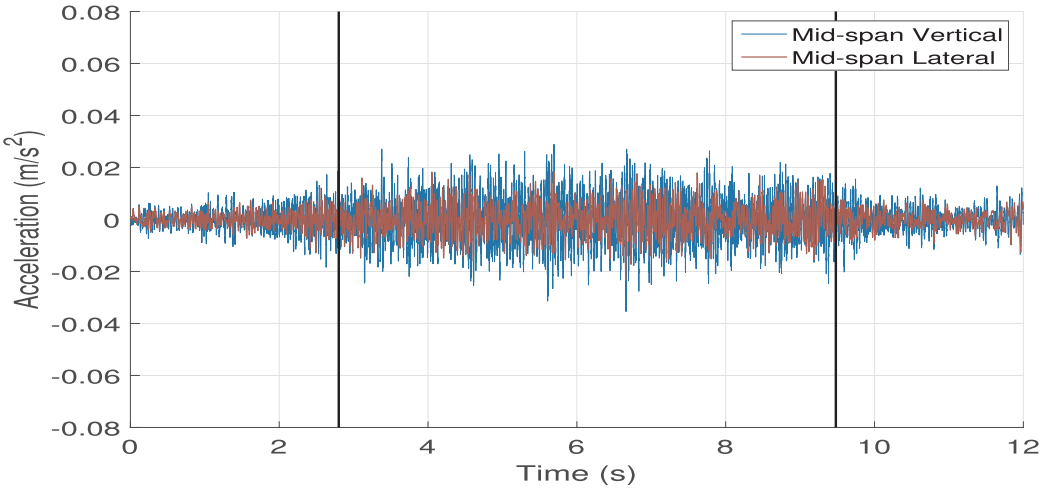

(b) Train 395-D-2 (16.8m/s)

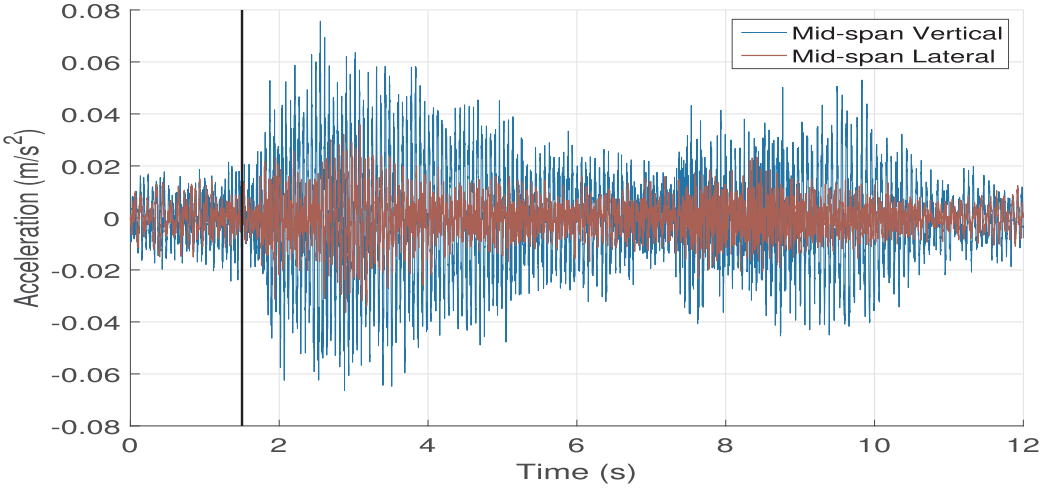

(c) Train 73/9-F-1 (10.7m/s)

Fig. 9. Vertical and lateral accelerations from three train passes including estimates of the timing of the train nose and tail passing beneath the bridge.

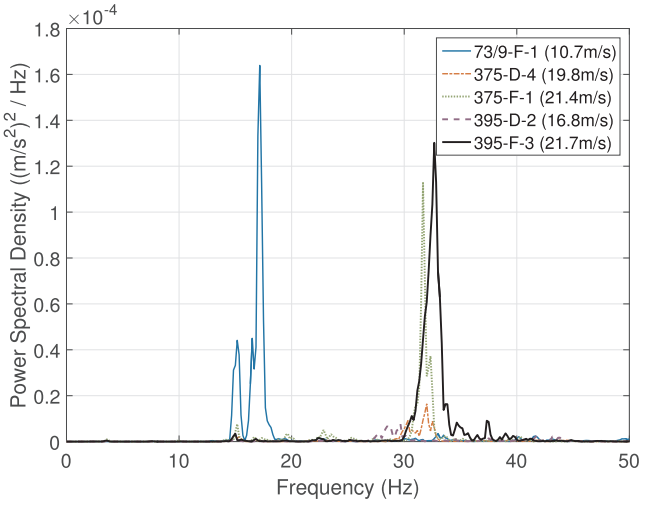

(a) Vertical mid-span acceleration

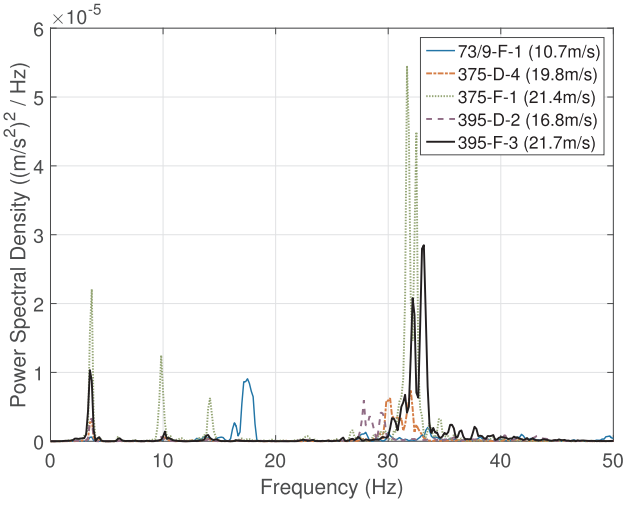

(b) Lateral mid-span acceleration

Fig. 10. PSDs of accelerations for different train passes.

As aerodynamic actions from passing trains onto structures are related to the square of the train speed, the inability of the trains to develop design line speeds leads to significant reduction in the pressures applied to the bridge, compared with the design value [11,27].

5.2. Vibration sources

Although it is known that there are excitation sources associated with train motion which can be transferred to a structure above the rail track, these are rarely commented in vibration analysis of footbridges. This section provides a reader with a rare insight based on experimental data. Fig. 8 shows the spectra of the vertical and lateral accelerations measured at the mid-span of the bridge as a train passes under. The strongest components in the 250–300 Hz range are caused by engine actions and wheel/track interactions [28]. This frequency range is too high to be perceptible by pedestrians. The audible sound of a train approaching also lies in this frequency range; as is confirmed by Fourier analysis of the audio recording from the camera. The strong peak around 30 Hz coincides with the sleeper frequency, f_s (in Hz) that represents the ratio between the train speed, v_t (in m/s), and sleeper spacing, L_s (in m) as given by Eq. 4 [10]:

$$f_s = \frac{v_t}{L_s} \tag{4}$$

This peak in the spectrum appeared at different frequencies for different train passes due to differences in the passing speed.

Next there is, in general, a train load frequency associated with the length of the carriage, or spacing between wheels [28,29]. For the range of speeds recorded this would give a frequency of around 1 Hz, however site conditions meant that this excitation effect was not felt on the bridge. Additionally, the peaks in the 50–100 Hz range are the result of other mechanical and rail interaction dynamics, but are outside the range of interest for structural assessment.

Finally, as a result of a nearby bend in the track towards Dover, all the trains were either accelerating or decelerating while passing under the bridge. This change in speed (of up to 2 m/s in 8 s) means there is not a unique excitation frequency associated with the train effects, but rather a time-dependant range.

5.3. Vibration response

The vertical and lateral mid-span accelerations for three different train passes are presented in Fig. 9. Each case was low-pass filtered at 40 Hz to remove the frequencies unlikely to be of interest to structural response or pedestrian comfort and the vertical lines indicate estimates for the train head and tail passing beneath the bridge based on pressure readings (with an exception of the train pass in Fig. 9(c) for which the end time could not be estimated). The train with the highest recorded speed (21.7 m/s), shown in Fig. 9(a), causes vibrations more than two times larger than one of the slowest cases (Fig. 9(b)), but at 21.7 m/s it takes less than six seconds for the six carriages of the train to pass, and the maximum measured accelerations are only for around 2 s of this. A different response is seen from the slow moving freight train in Fig. 9(c). Despite its much lower speed it is more effective at exciting the bridge, the reason behind this phenomenon will be clear from analysis of the spectrum of the acceleration response. Additionally, the effect of the two locomotive carriages at either end can be clearly seen, with a small lull period between them.

Further understanding of the different responses seen from different trains can be gained from the PSDs, plotted in Fig. 10(a) and (b) for vertical and lateral accelerations for five train passes representing different types and speeds of train. For these, a 12 s recording of the mid-span accelerations was taken and an average of three, six second long, Fourier Transforms made with an overlap of 50% and a Hanning window applied. Fig. 10(a) shows that the vertical acceleration observed from the higher speed trains (375-F-1 and 395-F-3; also see Fig. 9(a)) is predominantly based around the 30–35 Hz range with only a slight effect at the first vertical frequency of the bridge at about 15.1 Hz. The lower speed trains (395-D-2, also shown in Fig. 9(b), and 375-D-4) are even less effective at exciting the first vertical mode due to their lower excitation energy. The slowest freight train however, excited the first vertical mode the most, which might be counter-intuitive at first. Here the primary excitation frequency is at 17.2 Hz (see Fig. 10(a)), which is the sleeper frequency (Eq. 4). Since this excitation frequency is very close to the frequency of the first two vertical modes, it results in higher levels of vibration. If the train was travelling slightly slower the effect would be even worse. This response is similar to the effect demonstrated by Drygala et al. [4] where an even slower moving fright train caused the largest vibrations on a GFRP bridge with a lower natural frequency. Such effects emphasise the need to consider frequency content of both loading and the bridge in any dynamic analysis. Analysis of all the available data demonstrated that the supports also vibrated at frequencies in the 30–35 Hz range, corresponding to the sleeper spacing frequency, suggesting the transfer of the vibrations to the structure is through the ground.

The lateral response, shown in Fig. 10(b), demonstrates that many of the trains did energise multiple lateral modes up to 20 Hz, including the modes that were not present during the in-factory tests. However, as shown earlier in Fig. 9, the vibrations levels stayed very small.

Considering all the available train passes it can be concluded that no

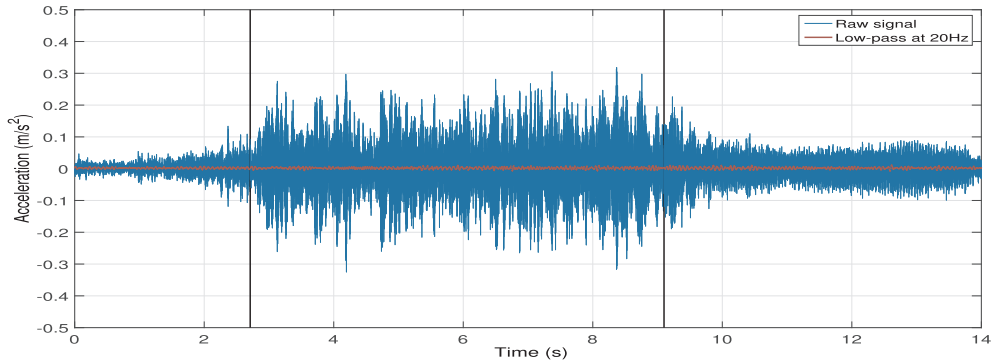

(a) Vertical mid-span acceleation

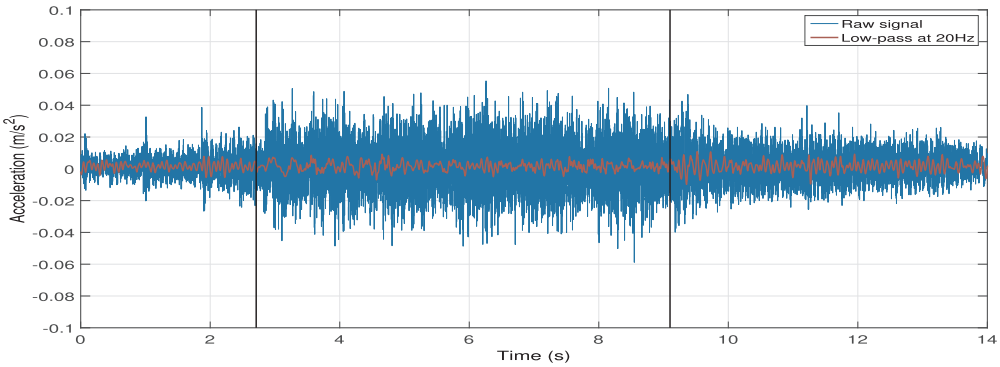

(b) Lateral mid-span acceleation

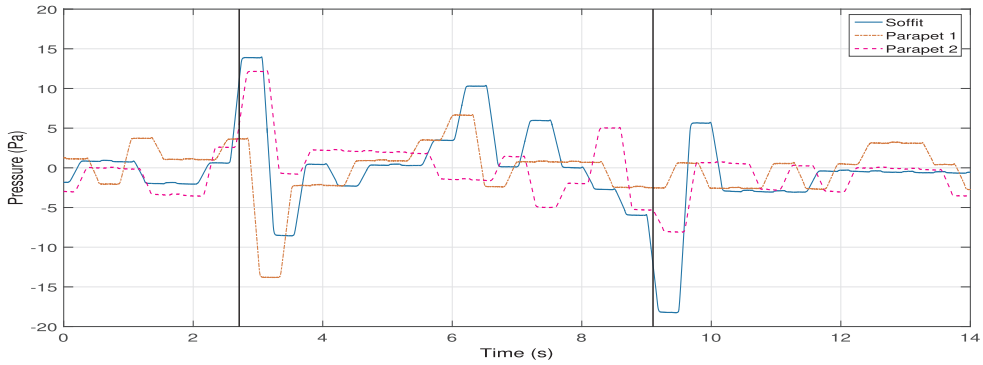

(c) Pressures

Fig. 11. Acceleration and pressure response from Train 395-F-1.

train caused large vibrations. Furthermore, there were no obvious patterns between speed, type or direction of the trains on the measured response. This is due to different contribution of different frequency components to the overall response, as demonstrated on the examples shown in Fig. 10.

As mentioned earlier there is currently a lack of experimental data for the effects of train buffeting on bridges, but some comparisons can be made. A similar study on a 12 m GFRP rail overbridge with a first vertical mode at 17.4 Hz and with trains travelling at 22.8 m/s (82.1 km/h, 51.0mph) resulted in peak vertical vibrations of 3.5 m/s^2 [15]. If these vibrations were at a low frequency, they would almost certainly have been considered as unacceptable by bridge users. However, the authors noted that these occurred at frequencies much higher than are perceptible to pedestrians. It is possible therefore that the observed vibrations were predominantly caused by mechanical vibrations travelling through the foundations rather than by buffeting, in which case they were unlikely to cause any concern. This example illustrates how important is to state frequency content of the vibration response caused by passing trains when interpreting the VSLS performance.

For consideration of the potential effect of train buffeting, the results from the differential pressure sensors were taken. As the sensors were chosen based on the full design pressure loading of 1 kPa predicted for the site in Eurocode 1 Part 2 [30], this meant they were not as accurate at measuring the low pressure effects that actually occurred in usage due to the reduced train speeds. However, they proved useful in identifying the moment of the positive peak at the head of the train, and the symmetrical response at the end and its influence on the vibration response of the bridge.

Fig. 11 gives an example of the results from a typical train. The vertical lines indicate the approximate timings of the pressure peaks in order to compare them to the vibration response. Additionally, both the

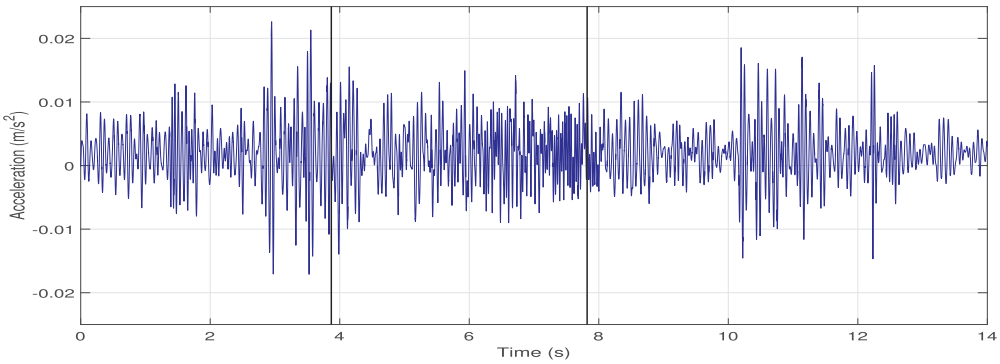

(a) Vertical mid-span acceleation

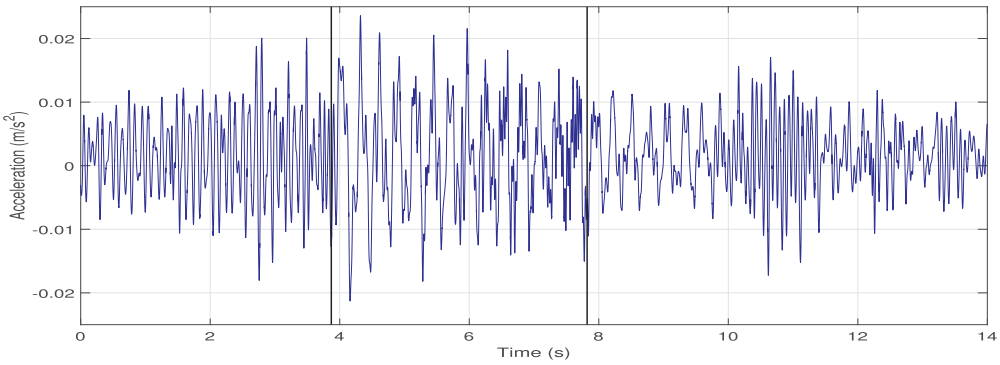

(b) Lateral mid-span acceleation

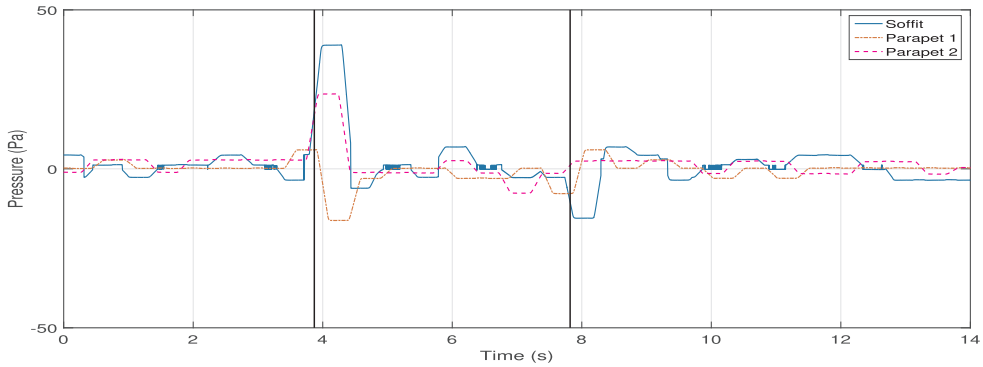

(c) Pressures

Fig. 12. Acceleration (20 Hz low-pass filtered) and pressure response from Train 375-F-1.

raw accelerations and a 20 Hz low-pass signal are presented to isolate potential influence of the train-generated wind from the ground excitations. It can be seen from the raw signal that the vibrations of the bridge start to develop before the buffeting hits, due to vibrations transmitted through the foundations as the train approaches. On the pressure response, there is a small, but detectable, effect on the underside and the sides of the bridge, but there is not a sudden change in the vertical acceleration response at this moment suggesting little vertical buffeting influence. The largest, low frequency lateral vibrations came from a fast but non-streamlined train, ID 375-F-1 (see Fig. 10(b)), for which aerodynamics effects would be expected to be the worst. Fig. 12 shows only the frequency components up to 20 Hz for this passage. It demonstrates a noticeable change in the frequency and amplitude of the lateral response coinciding with the arrival of the pressure wave. This effect appears to be a result of buffeting. Note that this train was only three carriages long, hence its shorter time record.

To conclude, the buffeting effect caused by the passage of the train exists on this bridge, but vibration levels remain small. Ground borne vibration from the train, mainly from its sleeper spacing frequency, dominates the response below 50 Hz. Separating the vibration that propagates to the structure through the ground from those that propagate through air is important because different frequency content causes different effects on how bridge will be perceived by pedestrians. For example, higher speed trains have higher associated excitation frequencies and so may be less significant for common structural ranges. On the other hand, as pressures due to train buffeting are non-linearly related to speed, faster trains could induce much higher buffeting effects which lightweight structures, such as GFRP footbridges, could be susceptible to.

6. Summary and conclusions

The dynamic properties of a 14.5 m GFRP truss bridge were investigated and the mode shapes and frequencies determined. Comparison to modal properties of the bridge before and after installation on site were made, demonstrating that while many modes remain similar, additional vibration modes appeared on site due to the specifics of the boundary conditions. This highlights that in-factory quality control tests for dynamic response must be conducted and interpreted with care to ensure suitable comparison with in-use behaviour.

To check vibration response to humans, single walker and crowd loading scenarios were applied to the bridge. It was demonstrated that this bridge has satisfactory vibration performance for these events. However, it has been shown that the minimum safe frequency limit recommended in design of footbridges against walking excitation based on experience with traditional construction materials is not directly transferable to lighter GFRP footbridges and it should be extended to account for excitation by higher harmonics of the dynamic force. As a result, design of GFRP bridges requires the use of models of the dynamic force that includes the frequency content up to about 17 Hz. A force model consisting of 12 harmonics, which is an extension of the ISO model, was proposed. It is demonstrated that this simple model results in good estimates of the vibration response.

With regard to train passing, the lower than expected speed of the trains reduced the aerodynamics effects to a very low level, but train-induced vibrations were measured. These were typically in the 30–40 Hz range and were carried through the ground, rather than the air. The absence of bridge modes in this frequency range was the reason that the acceleration response on the bridge was at a very low level. Pressure waves caused by the train passage did have a small effect on the bridge, especially on the lateral response, but a combination of the lower train speeds and the bridge properties meant buffeting effects were not significant. The results demonstrate that despite the lightweight and low stiffness nature of GFRP materials, there are no major vibration problems for the Dover Seawall Bridge caused by pedestrians or trains. This is a result of its good design and the specifics of the bridge location. This study shows that GFRP footbridges are a viable option for rail crossings. Additionally, the excellent vibration performance of this bridge offers opportunities for further design optimisation that could produce even more efficient structures without compromising vibration serviceability performance.

Data availability

Electronic format of the data collected in this research can be downloaded freely from the University of Warwick webpages wrap.warwick.ac.uk/136500.

CRediT authorship contribution statement

J.M. Russell: Conceptualization, Investigation, Software, Formal analysis, Writing - original draft. **X. Wei:** Investigation, Formal analysis, Writing - review & editing. **S. Živanović:** Supervision, Conceptualization, Validation, Writing - review & editing, Funding acquisition. **C. Kruger:** Writing - review & editing, Resources.

Declaration of Competing Interest

The authors declare that they have no known competing financial interests or personal relationships that could have appeared to influence the work reported in this paper.

Acknowledgements

This research work was supported by the UK Engineering and Physical Sciences Research Council [Grant No. EP/M021505/1: Characterising dynamic performance of fibre reinforced polymer structures for resilience and sustainability]. The authors would also like to thank Pipex px, Network Rail and Costain for their assistance with accessing and testing the bridge.

References

[1] Osborne J. On track to transform Europe's rail industry. Reinf Plast 2012;56:24–8.
[2] Wei X, Russell J, Živanović S, Mottram JT. Measured dynamic properties for frp footbridges and their critical comparison against structures made of conventional construction materials. Compos Struct 2019;223:110956.
[3] Živanović S, Feltrin G, Mottram J, Brownjohn J. Vibration performance of bridges made of fibre reinforced polymer. Dynamics of civil structures, vol. 4. Springer; 2014. p. 155–62.
[4] Drygala IJ, Polak MA, Dulinska JM. Vibration serviceability assessment of gfrp pedestrian bridges. Eng Struct 2019;184:176–85.
[5] Racic V, Pavic A, Brownjohn J. Experimental identification and analytical modelling of human walking forces: Literature review. J Sound Vib 2009;326:1–49.
[6] Shahabpoor E, Pavic A, Racic V. Interaction between walking humans and structures in vertical direction: a literature review. Shock Vib 2016;2016.
[7] Sétra F. Assessment of vibrational behaviour of footbridges under pedestrian loading. Technical guide SETRA, Paris, France; 2006.
[8] BSI, NA to BS EN 1991–2: 2003. UK National Annex to Eurocode 1: Actions on structures — Part 2: Traffic loads on bridges; 2008.
[9] ISO, ISO 10137: Bases for design of structure — Serviceability of buildings and walkways against vibrations; 2007.
[10] Kouroussis G, Connolly DP, Forde MC, Verlinden O. Train speed calculation using ground vibrations. Proc Inst Mech Eng Part F: J Rail Rapid Transit 2015;229:466–83.
[11] Baker C, Jordan S, Gilbert T, Quinn A, Sterling M, Johnson T, et al. Transient aerodynamic pressures and forces on trackside and overhead structures due to passing trains. part 1: Model-scale experiments; part 2: Standards applications. Proc Inst Mech Eng Part F: J Rail Rapid Transit 2014;228:37–70.
[12] Lombaert G, Degrande G, Kogut J, François S. The experimental validation of a numerical model for the prediction of railway induced vibrations. J Sound Vib 2006;297:512–35.
[13] Liu K, Reynders E, De Roeck G, Lombaert G. Experimental and numerical analysis of a composite bridge for high-speed trains. J Sound Vib 2009;320:201–20.
[14] Shave J, Denton S, Frostick I. Design of the St Austell fibre-reinforced polymer footbridge, UK. Struct Eng Int 2010;20:427–9.
[15] Santos FMd, Mohan M. Train buffeting measurements on a fibre-reinforced plastic composite footbridge. Struct Eng Int 2011;21:285–9.
[16] Russell J, Wei X, Živanović S, Kruger C. Dynamic response of an FRP footbridge due to pedestrians and train buffeting. Procedia Eng 2017;199:3059–64.
[17] FRP Specifications. Section 06 71 00 Fiberglass Reinforced Polymer (FRP) Structural Shapes/Plate and Fabrications, Strongwell, Strongwell Corporation, Bristol, Virginia; 2016.
[18] Fladung W. Windows used for impact testing. Proceedings-Spie The International Society For Optical Engineering. SPIE International Society for optics and photonics; 1997. p. 1662–6.
[19] Richardson MH, Formenti DL, Parameter estimation from frequency response measurements using rational fraction polynomials. In: Proceedings of the 1st international modal analysis conference, vol. 1, NY: Union College Schenectady; 1982. p. 167–86.
[20] Richardson MH, Formenti DL. Global curve fitting of frequency response measurements using the rational fraction polynomial method. In: Proceeding of 3rd IMAC; 1985. p. 390–7.
[21] Vibrant Technology, MEscope VES 6.0; 2013.
[22] MATLAB, version 8.6.0 (R2015b), The MathWorks Inc., Natick, Massachusetts; 2015.
[23] Richardson MH, Jamestown C. Modal mass, stiffness and damping. Jamestown, CA: Vibrant Technology, Inc.; 2000. p. 1–5.
[24] Grundmann H, Kreuzinger H, Schneider M. Dynamic calculations of footbridges. Bauingenieur 1993;68:215–25. [in German].
[25] Živanović S. Benchmark footbridge for vibration serviceability assessment under the vertical component of pedestrian load. J Struct Eng 2012;138:1193–202.
[26] Živanović S, Russell J, Pavlovic M, Wei X, Mottram JT. Effects of Pedestrian Excitation on Two Short-Span FRP Footbridges in Delft, IMAC-XXXVI, Orlando, Florida, 12–15 February; 2018.
[27] BSI, EN 14067-4: 2013. Railway applications — aerodynamics — Part 4: requirements and test procedures for aerodynamics on open track; 2013.
[28] Kouroussis G, Connolly DP, Verlinden O. Railway-induced ground vibrations–a review of vehicle effects. Int J Rail Transp 2014;2:69–110.
[29] Milne D, Le Pen L, Thompson D, Powrie W. Properties of train load frequencies and their applications. J Sound Vib 2017;397:123–40.
[30] BSI, BS EN 1991–2: 2003. Eurocode 1: Actions on structures — Part 2: Traffic loads on bridges; 2003.